Aalborg Universitet

AALBORG UNIVERSITY

DENMARK

An Experimental Study of a Midbroken 2-Bay 6-Storey Reinforced Concrete Frame subject to Earthquakes

Skjærbæk, P. S.; Taskin, B.; Kirkegaard, Poul Henning; Nielsen, Søren R. K.

PII: S 0267-7261(97)00013-4

An experimental study of a midbroken 2-bay, 6-storey reinforced concrete frame subject to earthquakes

P.S. Skjærbæk[a], B. Taşkin[b], P.H. Kirkegaard[a] & S.R.K. Nielsen[a]

[a]*Department of Building Technology and Structural Engineering, Aalborg University, DK-9000 Aalborg, Denmark*
[b]*Civil Engineering Faculty, Department of Structural Engineering, İstanbul Technical University, 80626 Maslak, İstanbul, Turkey*

A 2-bay, 6-storey model test reinforced concrete frame (scale 1:5) subjected to sequential earthquakes of increasing magnitude is considered in this paper. The frame was designed with a weak storey, in which the columns are weakened by using thinner and weaker reinforcement bars. The aim of the work is to study the global response to a damaging strong motion earthquake event of such buildings. Special emphasis is put on examining to what extent damage in the weak storey can be identified from global response measurements during an earthquake where the structure survives, and what level of excitation is necessary in order to identify the weak storey. Furthermore, emphasis is put on examining how and where damage develops in the structure and especially how the weak storey accumulates damage. Besides the damage in each storey the structure is identified by a static load at the top storey while measuring the horizontal displacement of the stories and also visual inspection is performed. From the investigations it is found that the reason for failure in the weak storey is that the absolute value of the stiffness deteriorates to a critical value where large plastic deformations occur and the storey is not capable of transferring the shear forces from the storeys above so failure is unavoidable. © 1997 Elsevier Science Limited.

Key words: model testing, reinforced concrete structures, damage assessment, modal identification, midbroken structures.

1 INTRODUCTION

Dynamic loads seen in nature such as earthquakes, winds, floods, etc. cause damage to civil engineering structures. Since there is no escape from this reality, the only thing that can be done for an existing structure is to control the growth of damage by suitable localization and quantification procedures. In most earthquake codes, the acceptable level of damage is specified depending on the strength of the earthquake, but the main idea is to prevent total collapse of a structure or total collapse of a part of a structure and make it repairable, so the demolition of the structure can be avoided. This point of view led to a new research area known as 'damage assessment' resulting in many different methods in the literature in the last 10–20 years.

In reinforced concrete (RC) structures, damage under dynamic loadings usually starts as cracks followed by crushing of concrete or yielding of reinforcement, in the case that the structure does not suffer any other kind of construction failure. Traditionally, assessment of damage in RC-structures is made by visual inspection of the structure by measuring cracks, permanent deformations, etc. This is often very cumbersome, since panels and other walls covering beams and columns need to be removed. However, developments in earthquake engineering and especially developments in the last 10–20 years of damage assessment procedures, offer a much more attractive method which basically depends on measuring the structural response at given locations of the structure. Almost all of the methods developed according to this idea are based on calculating a so-called damage index, which is supposed to reflect the damage state of the considered structure, substructure or structural member by the use of e.g. changes in dynamic characteristics. In the literature, several methods for damage
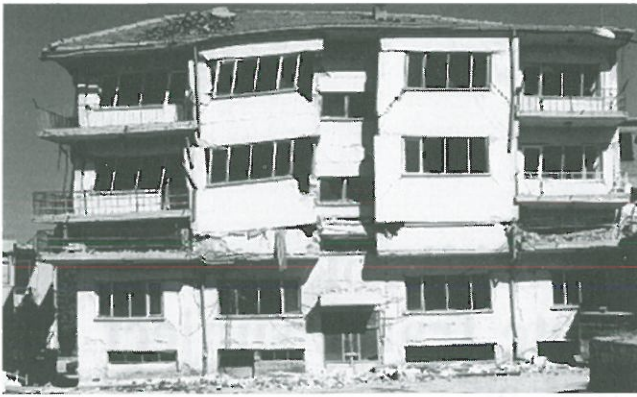
Fig. 1. Collapse of an intermedia floor due to the October 1995 Earthquake, Dinar, Turkey.

assessment from measured responses have been presented during the last two decades [1–10,3,11 12–17].

Recent earthquake events have revealed a class of structures which can be referred to as midbroken structures (pancake type of damage). As a definition, a midbroken structure has a storey weakened by some kind of change in the material used or changes in the geometry of members' cross-sections. Examples of this phenomenon are found in Turkey and Greece, where buildings are often built in several stages. After the construction of each stage, reinforcement

bars are left extended through the next storey and finally through the concrete deck at the roof. When the construction work is resumed, perhaps years later, these extended reinforcement bars are used to connect and anchor the new stuctural components to the existing building. Recent earthquake events in Turkey and Greece have shown that such structures have a tendency to fail in the storeys where such a connection is performed. The same kind of failure mode was also seen in the Kobe 1995 earthquake, where mid-storey collapses were caused by a sudden change in stiffness and strength of the storey columns. An example of such a failure can be seen in Fig. 1.

Until now only very limited research has been dedicated to this phenomenon, and the studies have been limited to numerical simulation studies by e.g. Skjærbæk et al. [18] and Köylüoğlu et al. [19,20]. The results of these simulations indicate that the increased amount of damage in a weak storey is mainly due to the strength degradation. However, some divergence has been found between different models used in the simulations, and experimental verification of the simulated results is desired.

The aim of this paper is to present an experimental investigation on the effect of a weak storey in a structure. Special emphasis is put on investigating to what extent the weak storey can be identified from global response measurements during an earthquake where the structure survives,
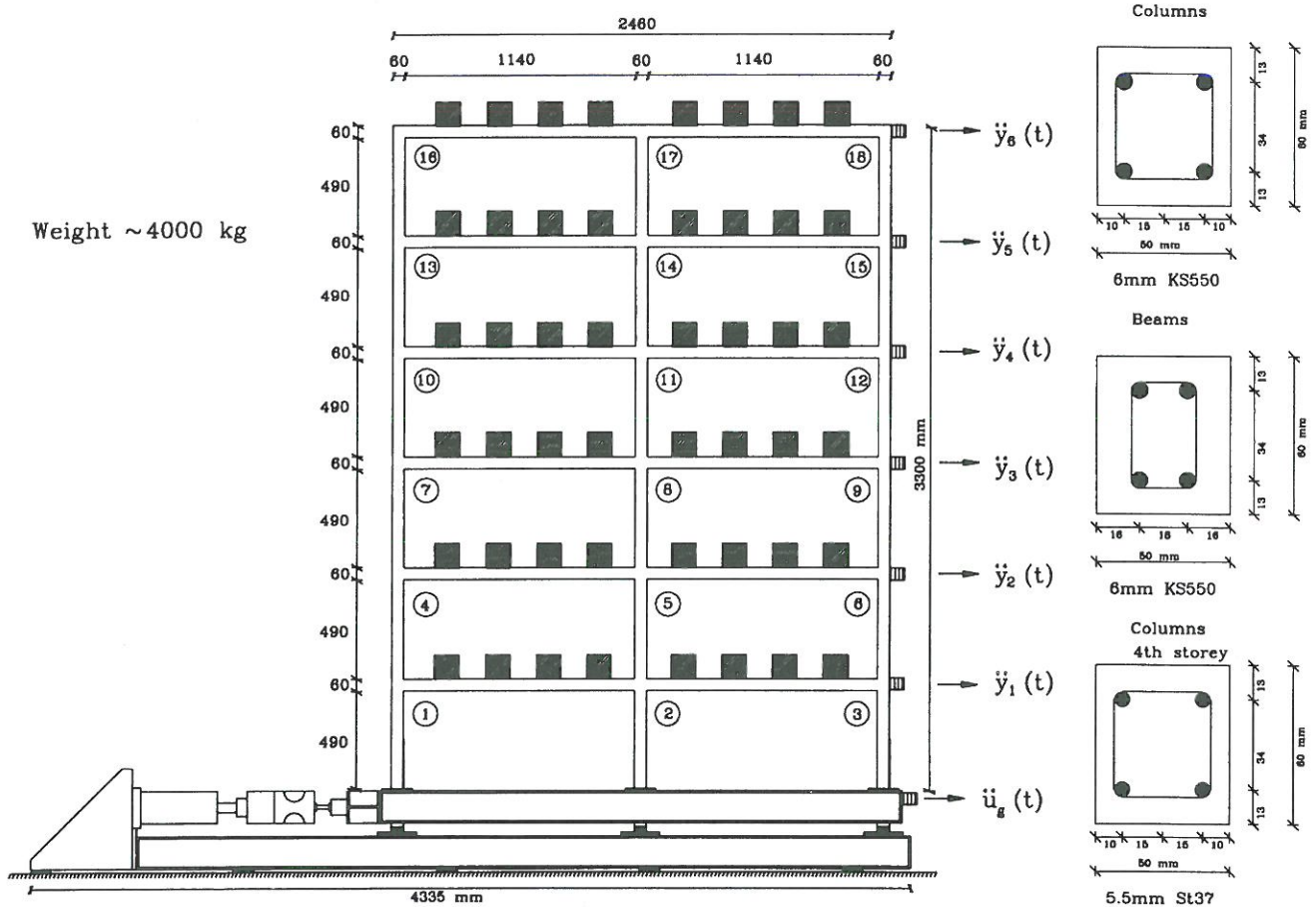

Fig. 2. Plane view of experimental set-up and cross-sections of beams and columns.
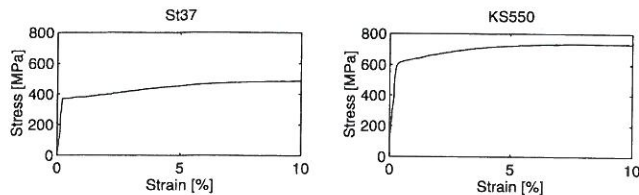
Fig. 3. Stress–strain curves for the used types of reinforcement.

and to investigate why the weak storeys seem to fail during earthquakes.

2 THE TEST STRUCTURE

For the test series two reinforced concrete frames were cast one at a time and were constructed identically. The test frame considered is a 6-storey, 2-bay RC-frame. The dimensions of the test frame are 2460 by 3300 mm corresponding to a 'real' structure with dimensions 12.3 by 16.5 m. The test frame is built of 50 by 60 mm RC-sections constant all over the frame. The weight of each frame is ≈2 kN. To model the storey deck, 8 RC beams (0.12 × 0.12 × 2.0 m) are placed on each storey. The total weight per frame is then ≈20 kN which makes about 40 kN in total for the test structure.

The longitudinal reinforcements used in the frame are of type KS550 (ribbed steel) with an average yield stress of 610 MPa. In the weak fourth storey St37 steel bars were used with an average yield strength of 390 MPa. Columns and beams are reinforced with 4Φ6 KS550 and in the weak storey, columns are reinforced with 4ø5.5 St37. A plane view of the test frame and the reinforcement of the cross-sections can be seen in Fig. 2(a) and (b) respectively.

In Fig. 3(a) and (b) typical stress–strain curves are shown for the two types of steel.

To avoid overlapping in the longitudinal reinforcement giving uncontrolled changes in bending stiffness and strength, the ends of the longitudinal reinforcement bars are provided with anchoring steel-plates welded to the reinforcement.

The concrete used has a design compression strength of 30 MPa with a maximum aggregate diameter of 5 mm. The ultimate stress determined from test cylinders' compression tests is approximately $f_c = 45$ MPa.

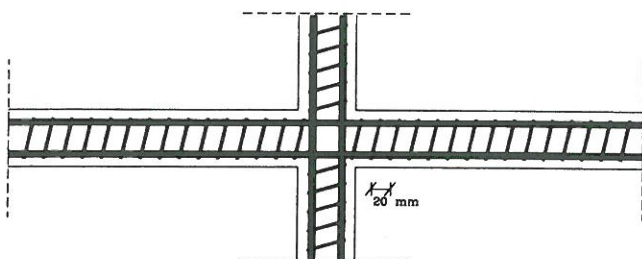All columns and beams are reinforced against shear with

2 mm steel thread which has been formed into spirals, as seen in Fig. 4.

3 TEST SET-UP AND CONDUCTION OF DYNAMIC TESTS

The frames are tested in pairs of two where the same ground surface acceleration is applied to the two frames. The frames are placed at the shaking table at a distance of 1000 mm and are stabilized in space by a steel cross at each end. In the connection between the shaking table and the hydraulic cylinder a load cell is placed to measure the actual cylinder force as a function of time. Furthermore, the cylinder is capable of measuring the cylinder displacements as a function of time. Both the right- and the left-hand frames were equipped with an accelerometer measuring the horizontal acceleration at each of the storeys. Also the shaking table is equipped with an accelerometer measuring the horizontal ground accelerations. Furthermore, a load-cell and a displacement transducer are attached to the hydraulic cylinder measuring the applied force and the ground displacements, Fig. 2(a).

3.1 Non-destructive testing

The non-destructive testing is performed by means of free decay tests in which a horizontal force at the top storey of the frame is applied and where the structure is identified from well defined data. Free decay tests are performed in the virgin state of the structure and subsequent to each of the earthquake events.

3.2 Destructive testing

The destructive testing is performed by applying three sequences of earthquake-like ground motions to the model test structure. The acceleration vs. time diagrams are given in Fig. 5.

The time series shown in Fig. 5 were generated by filtering white noise through a Kanai-Tajimi filter with a circular
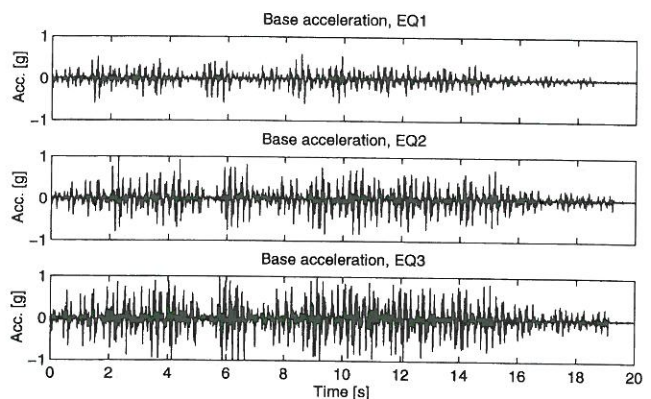

Fig. 4. Shear reinforcement of columns and beams.

Fig. 5. The three applied earthquakes.

Table 1. Estimated modal parameters for virgin frame AAU4

Method	State	f_1 (Hz)	f_2 (Hz)	ζ_1 (%)	ζ_2 (%)
ARV	0.25 kN	2.68	8.66	1.12	0.54
ERA	0.25 kN	2.68	8.66	1.14	0.35
POLYREF	0.25 kN	2.67	8.66	1.19	0.70
ARMAV	0.25 kN	2.68	8.66	1.24	0.51
Average	0.50 kN	2.64	8.58	1.35	0.82
Average	0.75 kN	2.62	8.51	1.48	0.99

Table 2. Estimated modal parameters of frame AAU4 after EQ1

Method	State	f_1 (Hz)	f_2 (Hz)	ζ_1 (%)	ζ_2 (%)
Average	0.25 kN	2.31	7.46	2.15	1.44
Average	0.50 kN	2.22	7.18	2.92	1.90
Average	0.75 kN	2.16	7.01	3.22	1.94

frequency of 30 rad s^{-1} and a damping ratio of 0.1. This centre frequency is likely to excite primarily the first and second modes of the structure.

4 NON-DESTRUCTIVE DYNAMIC TESTING

In this section the results of the non-destructive testing of the frame in the virgin state and the results after each strong motion event are presented. Before strong motions are applied the frame is subjected to various loads in the linear range to provide data for modal identification of the original structure. Furthermore, free decay tests are performed after each earthquake to provide 'clean' data for identification of the damaged structure. The frame is subjected to free decays of pull-outs in bending where a load of 0.25 kN, 0.50 kN, 0.75 kN has been applied step by step.

The free decay test time series were analysed using an AutoRegressive Vector model (ARV), Eigen Realization Algorithm (ERA), the Polyreference method (POLYREF) and an AutoRegressive Moving Average Vector (ARMAV) model, see Pandit [21], Juang [22], Vold [23] and Kirkegaard [24].

The modal parameters listed in Tables 1–4 were obtained with respect to the virgin state and after EQ1, EQ2 and EQ3 respectively. In Table 1, the results are listed for all four

methods in the case of a pull-out force of 0.25 kN and it can be seen that in case of frequencies all methods practically give the same results. The estimation of the damping ratios seems to be somewhat poorer. The remaining estimates of the modal parameters are listed as averages of the results obtained by the four methods.

From Tables 1 and 2 it can be seen that the frequency drops by approximately 14% after EQ1 while the damping ratio increases by approximately 100%. These values are 35% and 400% respectively after EQ2, and 45% and 350% respectively after EQ3, which is also obvious from Fig. 6.

As an example the top storey acceleration vs. time diagrams are plotted after each of the four types of loadings and can be seen in Fig. 6.

Using the the four presented methods it is possible to obtain estimates of the mode shapes as well. The results of the mode shape identification of the virgin structure and of the damaged structure after each earthquake are shown in Fig. 7 for a pull-out force of 0.5 kN using the ARV method.

No significant changes in the mode shapes were obtained after any of the earthquake events, as indicated in Fig. 7. Although there is a weak storey in the structure the mode shapes seem to be insensitive to even large stiffness changes.

Table 3. Estimated modal parameters of frame AAU4 after EQ2

Method	State	f_1 (Hz)	f_2 (Hz)	ζ_1 (%)	ζ_2 (%)
Average	0.25 kN	1.89	5.91	3.13	2.62
Average	0.50 kN	1.78	5.59	3.85	3.63
Average	0.75 kN	1.72	5.43	4.59	4.48

Table 4. Estimated modal parameters of frame AAU4 after EQ3

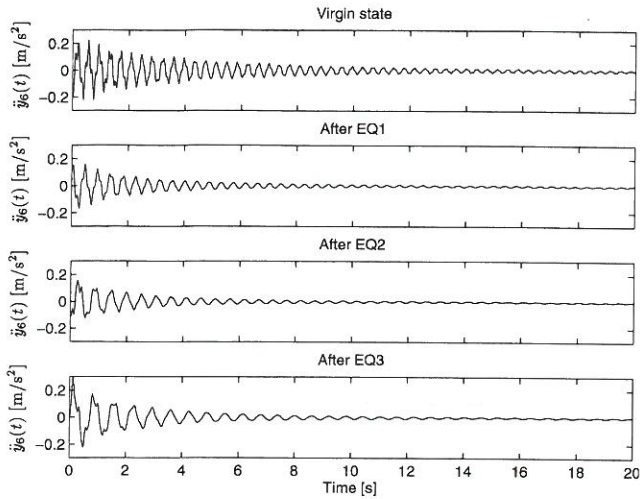| Method	State	f_1 (Hz)	f_2 (Hz)	ζ_1 (%)	ζ_2 (%)
Average	0.25 kN	1.55	4.83	3.52	2.27
Average	0.50 kN	1.42	4.50	5.11	3.06
Average	0.75 kN	1.38	4.36	4.52	3.30

Fig. 6. The top storey acceleration vs. time diagrams from the free decay tests: (a) undamaged structure, (b) after EQ1, (c) after EQ2 and (d) after EQ3.

5 DESTRUCTIVE DYNAMIC TESTING

In this section data collected during and after the strong motions applied to the structure are presented. In the destructive testing the frame AAU4 is exposed to three sequential earthquakes of increasing amplitude called EQ1, EQ2 and EQ3. In Fig. 8, measured accelerations at the top storey during the three earthquakes can be seen.
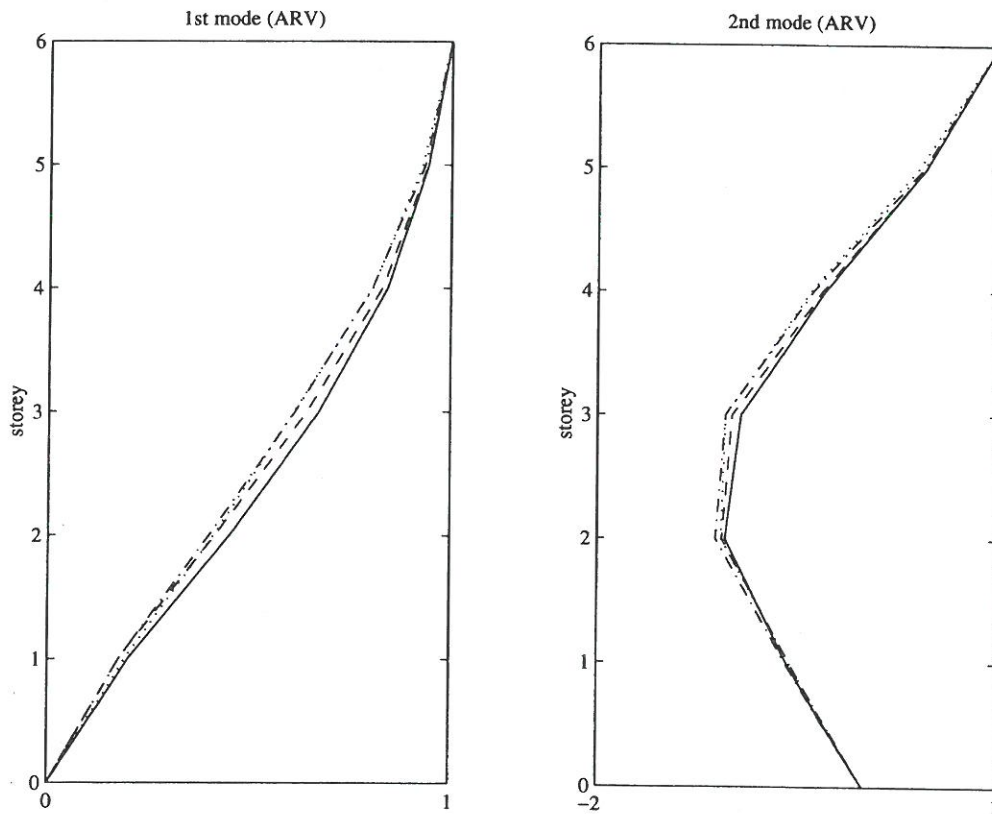
5.1 Processed data

This section presents processed data where inter-storey and top-storey displacements have been found using double time integration procedures as described in e.g. Skjærbæk [18]. During the integration process where displacements are obtained, a Butterworth 6th order high-pass digital filter with a cut-off frequency of 0.95 Hz and a Butterworth 8th order low-pass digital filter with a cut-off frequency of 20 Hz have been used. Furthermore, time series of eigen-frequencies are extracted from the strong motion records. The procedure for frequency estimation is described in Kirkegaard *et al.* [25]. In Fig. 9 the top storey displacements during EQ1, EQ2 and EQ3 are shown.

The displacement time series shown in Fig. 9 indicates that the global structural response during EQ1 is very small since the top storey displacement is smaller than 10 mm. As the structure becomes more damaged and the amplitude of the earthquake increases, it is seen that the global structural response is increasing quite dramatically.

In the same manner as for the top storey displacements, the interstorey drifts are evaluated and these are shown in Figs 10–12 for the three earthquakes respectively.

The interstorey displacements shown in Fig. 10 indicate that the main response is within the second, third and fourth storeys where the largest amplitudes are found. Especially, the response of the sixth storey is very limited and any damage observed in this storey is likely to be due to cracking of hitherto uncracked sections.
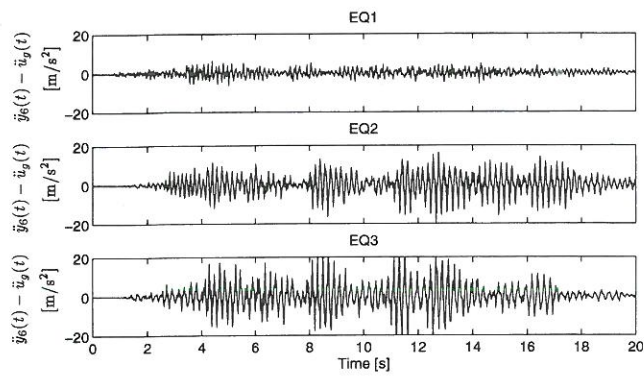

Fig. 7. Mode shapes of the structure: ——————, virgin state; - - -, after EQ1, − · −, after EQ2; · · · after EQ3.

Fig. 8. Top storey accelerations relative to ground surface during the three earthquakes.

During EQ2 the interstorey displacements increase significantly in all storeys and only the third storey seems to have significantly smaller amplitudes than the rest of the storeys. The maximum interstorey drift is found to be 10 mm in storey 5.

In the third earthquake the interstorey displacements increase further but the same distribution as during EQ2 is found between the storeys. So, based on the observed interstorey displacements the weak storey cannot be found, since no significant increase in interstorey displacements is observed.

In order to evaluate the development of the natural frequencies of the structure during the earthquakes a recursive implemented ARMAV model has been fitted to the measured acceleration time series, see Kirkegaard et al.[25]. In Fig. 13 the development in the two lowest eigenfrequencies of the structure are shown.

For each of the eigenfrequency time series the maximum softening damage index is evaluated. This index has proven to be a good measure of the global damage state of a reinforced concrete structure [26–28]

Generally the multi-dimensional maximum softening $\delta_{\mathrm{M},i}$ is defined according to Nielsen et al. [27] as

$$\delta_{\mathrm{M},i} = 1 - \frac{T_{i,\text{initial}}}{T_{i,\max}} \tag{1}$$

Where $T_{i,\text{initial}}$ is the initial value of the ith eigenperiod for

Fig. 10. Interstorey displacements during EQ1 for frame AAU4.

the undamaged structure and $T_{i,\max}$ is the maximum value of the ith eigenperiod during the earthquake. Fig. 13 also shows the plot of the damage curve $\delta_i(t) = 1 - T_{i,\text{initial}}/T_i(t)$, where T_i is the instantaneous eigenperiod.

DiPasquale et al. [5] investigated a series of buildings damaged during earthquakes and found a very small variation coefficient for the maximum softening damage index, see Fig. 14.
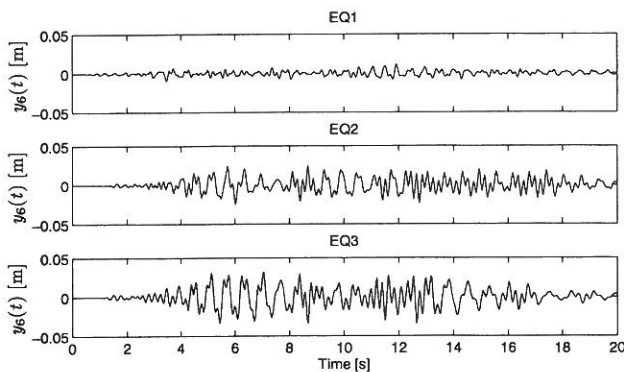

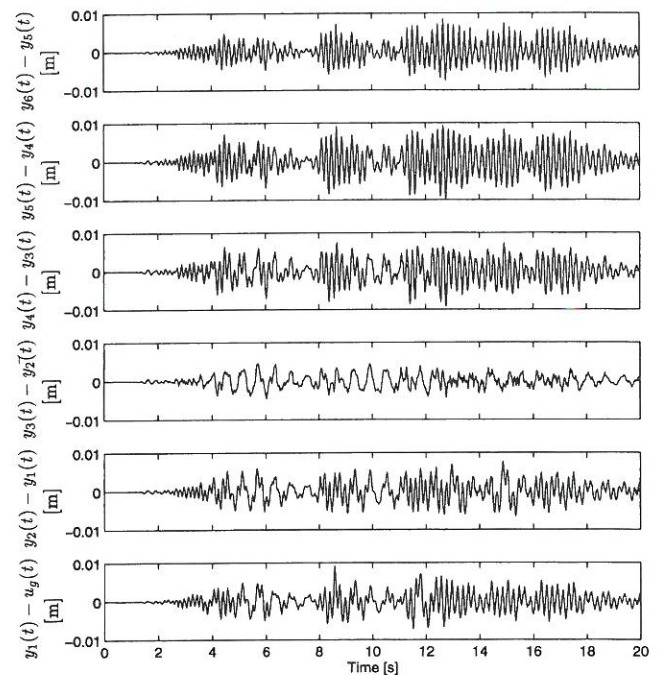**Fig. 9.** Top storey displacements relative to ground surface during EQ1, EQ2 and EQ3.

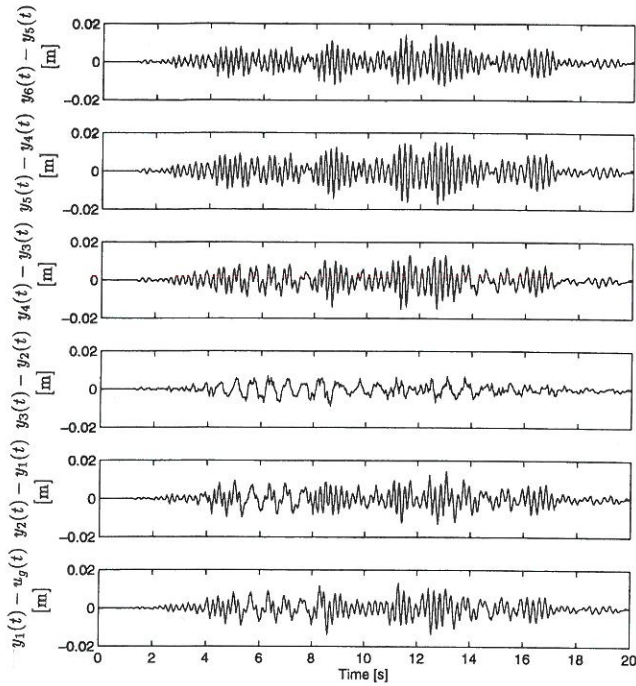**Fig. 11.** Interstorey displacements during EQ2 for frame AAU4.

Fig. 12. Interstorey displacements during EQ3 for frame AAU4.

The maximum softenings during the three runs are shown in Table 5.

6 STATIC TESTS

In order to evaluate the distribution of the damage, the structure is exposed to static tests after each earthquake event. The tests were performed with the entire structure.

In the static tests, a definite force is applied at the top storey and the displacements are measured at each storey.
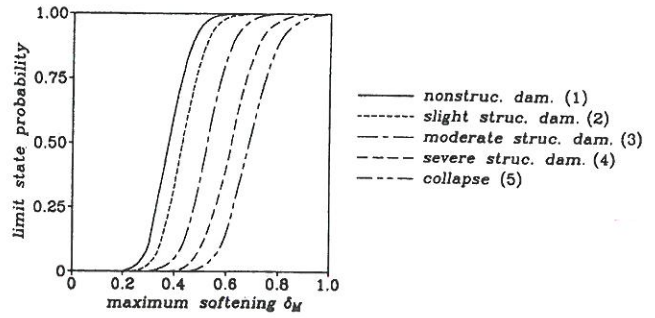

Fig. 14. Distribution function of observed limit state values of one-dimensional maximum softening reported by DiPasquale *et al.* [5]

The force is varied between 0 to 0.75 kN. A schematic view of the test set-up is shown in Fig. 15.

The static testing was performed on the entire structure in the virgin state, EQ1, EQ2 and EQ3. The results of all the static tests are shown in Fig. 16.

As seen from Fig. 16, the inter-storey displacement of the fourth storey is about 2.5 times higher than the avarage of the rest of the storeys in the virgin state, 2.7 times higher after EQ1, and 2.5 times higher after EQ2. As expected, the deformations increase significantly after EQ3. It should be noted that there is also soft behaviour at the top storey after EQ3 but still the relative displacement of the fourth storey is about 2.2 times higher than the average displacement value of the rest of the storeys. In Table 6, the stiffnesses found for each of the storeys are shown for the virgin structure as well as the structure after EQ1, EQ2 and EQ3.

Based on the stiffnesses determined in Table 6, a damage indicator $\delta_{S,i}$ for the ith storey can be represented as

$$\delta_{S,i} = 1 - \sqrt{\frac{K_{\text{final},i}}{K_{0,i}}} \qquad (2)$$
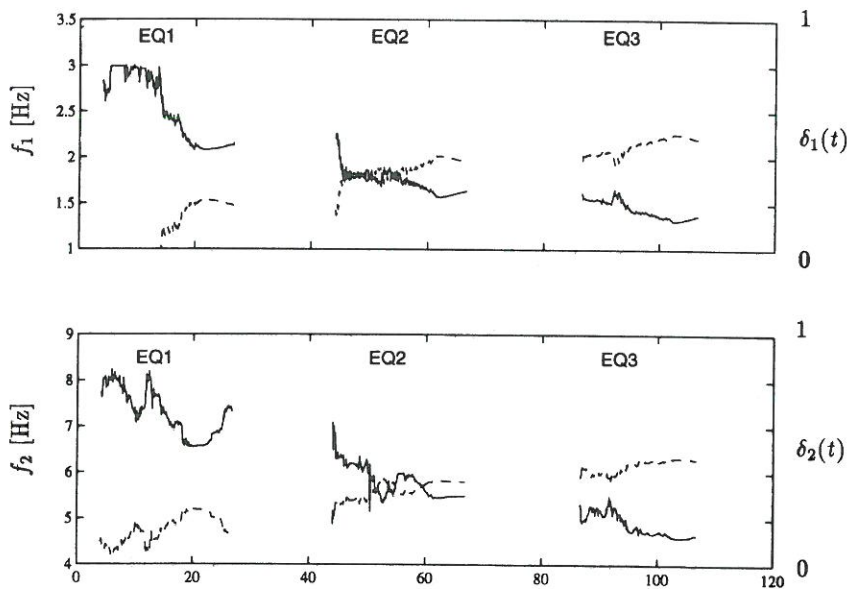

Fig. 13. Development of natural eigenfrequencies in the first and second modes and damage indices during EQ1, EQ2 and EQ3.

Table 5. Estimated minimum frequencies and maximum softenings during the three earthquakes

	$f_{\text{min},1}$ (Hz)	$f_{\text{min},2}$ (Hz)	$\delta_{\text{M},1}$	$\delta_{\text{M},2}$
EQ1	2.07	6.54	0.22	0.24
EQ2	1.57	5.15	0.41	0.40
EQ3	1.31	4.49	0.50	0.48

where $K_{0,i}$ is the apparent stiffness of the *i*th storey of the undamaged structure and $K_{\text{final},i}$ is the apparent stiffness of the *i*th storey after the forcing event. It should be noted that this formulation of the damage index, $\delta_{S,i}$, is compatible with the maximum softening index according to Nielsen *et al.* [27,28].

The damage indicators calculated after each earthquake event according to this criterion are listed in Table 7.

The damage indicator calculated for the sixth storey after EQ1 shows a very high damage level compared with the other storeys. This can be explained by the fact that the initial stiffness obtained from the pull-out tests of the storey is very high, which indicates that the elements in this storey are still uncracked although the other storeys are cracked. This interpretation is also supported by studying the observed inter-storey drifts during EQ1 in the sixth storey, where only very small deformations are found. Based on this assumption new damage indicators for the sixth storey are found to be $\delta_{S,6}^{\text{EQ1}} = 0.00$, $\delta_{S,6}^{\text{EQ2}} = 0.13$ and $\delta_{S,6}^{\text{EQ3}} = 0.40$.

In Fig. 17, the total deformations for each storey at the maximum load level are shown.

It is seen that the relative change in stiffness is approximately proportional in all storeys which also is supported by the evaluated mode shapes which remained almost unchanged. However, the absolute stiffness reduction in the weak storey leads to large plastic deformations appearing as damage in the structure. It is concluded that failure occurs when the stiffness reaches a critical value and the storey is no longer capable of transferring the shear forces from the storeys above.

7 VISUAL INSPECTION OF TEST STRUCTURE

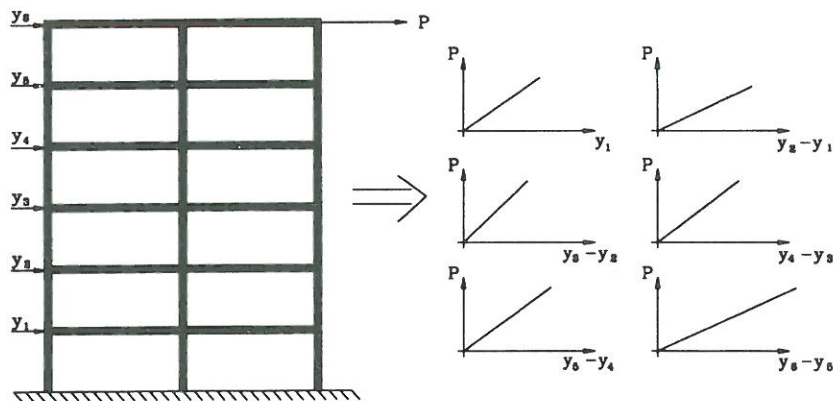After each of the strong motion loads, the structure was

Fig. 16. Force–deformation curves for interstorey displacements obtained from the static tests of the frame: ————, virgin structure; - - -, after EQ1; – · –, after EQ2; · · · after EQ3.

thoroughly examined visually by means of a magnification glass; all cracks were marked with different colours.

7.1 Definition of the classifications

After each series of ground motions the structure was thoroughly examined visually and the damage state of each storey of the building is classified into one of the following six classifications: undamaged (U), cracked (CR), lightly damaged (LD), damaged (D), severely damaged (SD) or collapse (CO). Each of the six classifications is defined in Table 8.

7.2 Damage assessment of frames AAUWa–b

Generally the cracks/damage were concentrated at the

Fig. 15. Static test set-up used for determination of lateral stiffness.

Table 6. Evaluated stiffnesses of the six storeys

Storey	Virgin (N mm^{-1})	EQ1 (N mm^{-1})	EQ2 (N mm^{-1})	EQ3 (N mm^{-1})
1	1499	1390	1010	932
2	2124	1456	1054	622
3	1870	1326	991	622
4	778	554	431	334
5	1486	1486	895	592
6	3339	1544	1160	548

Table 7. Calculated damage indices after each earthquake

Storey	$\delta_{S,i}$ (EQ1)	$\delta_{S,i}$ (EQ2)	$\delta_{S,i}$ (EQ3)
1	0.04	0.18	0.21
2	0.17	0.30	0.46
3	0.16	0.27	0.42
4	0.16	0.26	0.34
5	0.00	0.22	0.37
6	0.32	0.41	0.59

beam–column junctions at all load levels and the inspection was therefore concentrated at the nodes. After earthquake 1 (EQ1), the inspection of the nodes showed no serious cracks other than mostly micro-cracks. Only the nodes 2, 12 and 18 of frame AAUWb had shear cracks, not more than 0.02 mm wide. These cracks increased in length after EQ2 and also new shear cracks occurred at nodes 8 and 18 of frame AAUWa and 1, 8 and 15 of frame AAUWb. So the general impression from these visual inspections after EQ1 and EQ2 was that the damage was limited since only small cracks and some reasonable shear-cracks were present.

EQ3 resulted in some heavy damage at the nodes of the second and the fourth storeys which can be seen from the pictures in Fig. 18. Other than this heavy damage, most of the nodes had significant shear cracks. All three columns of the fourth storey of frame AAUWb had horizontal shear cuts where the maximum shear force is supposed to be. Storey 2 also had the same kind of damage.

There was no total or partial collapse after any of the earthquake events. However, the nodes 2, 11 and 14 of the frame AAUWa and the nodes 2, 11 and 14 of AAUWb can be presented as hinges. An overview of these visual inspections is given in Table 9.

It is quite clear from Table 9 that the first, fourth and the fifth storeys are the most damaged, while storey six has the least damage. In particular, the shear cuts seen in all three columns of the fourth storey prove that this storey has weaker columns than the others and the columns are almost in the ultimate limit state of their load bearing capacity.

8 SUMMARY

The results of a series of shaking table tests with a scale of 1:5, 6-storey reinforced concrete frame designed with a weak fourth storey have been presented. Initially the structure was exposed to various non-destructive tests in order to identify both inter-storey stiffnesses and modal parameters of the virgin structure. Afterwards three sequential earthquakes of increasing amplitude were applied to the structure. After each of the earthquake events the structure was again exposed to non-damaging tests to evaluate changes in inter-storey stiffness and modal parameters. From the strong motion measurements the two lowest time varying eigenfrequencies of the structure were estimated as functions of time, and the maximum softening was evaluated for the two modes. After the first earthquake (EQ1) sequence the maximum softening was evaluated at 0.22 and 0.24 in the first and second modes respectively. According to the fragility
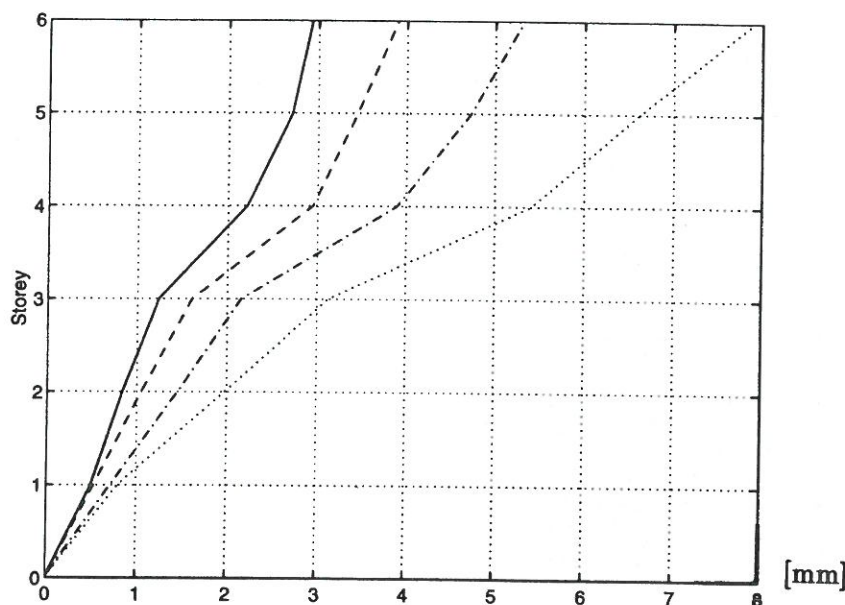

Fig. 17. Total deformations at maximum load. ————, virgin structure; - - -, after EQ1; – · –, after EQ2; · · · after EQ3.

Table 8. Definition of the six damage classifications used

Category	Definition
Undamaged UD	No external sign of changed integrity of any of the columns or beams in the storey
Cracked CR	Light cracking observed in several members but no permanent deformation
Lightly damaged LD	Severe cracking observed with minor permanent deformations
Damaged D	Severe cracking and local large permanent deformations observed
Severely damaged SD	Large permanent deformations observed and spalling of concrete at some members
Collapse CO	Very large permanent deformations observed and severe spalling of concrete at several members

curves for the maximum softening damage index presented in the literature this level for the maximum softening corresponds to only 'non-structural damage'. Visual inspection of the structure after the first earthquake only revealed development of a few micro-cracks in all storeys other than the fifth. The static testing of the storeys revealed stiffness changes in the four lower storeys and the sixth storey, where the stiffness change in the sixth storey can be referred to internal cracking since the response measurements only showed a very low level of inter-storey displacements in this storey. The mode shapes identified after the first earthquake were only found to change slightly, whereas the structural damping ratio in both the first and the second modes increased by approximately 100%.

After the second earthquake (EQ2) a maximum softening of 0.40 and 0.41 was found in the first and the second modes respectively. According to the fragility curves this corresponds to a 'light to moderate damage' state of the structure. The visual inspection revealed cracking spread out in the

entire structure and light damage was observed in the beam–column junctions above the first and the third storeys. The static tests showed stiffness changes in all storeys with the highest level in the second, third and fourth storeys. Again the identified modeshapes only revealed small changes but damping ratios were increased approximately 300% compared with the virgin structure. After the third earthquake (EQ3) a maximum softening of 0.50 and 0.48 was found in the first and second modes respectively, and this level coresponds to 'severe damage' in the structure. The visual inspection revealed severe damage with crushing of concrete in the beam–column junctions above the first, fourth and fifth storeys, whereas the static tests showed the largest reduction in stiffness in the second, third and sixth storeys. However, in none of the applied methods for damage assessment was the weak fourth storey found to be significantly more damaged than any of the other storeys, even though both the stiffness and strength of this storey were significantly lower than that of the other storeys in the virgin structure. No significant change was found in the mode shapes from EQ2 to EQ3 and the damping ratios remained at a level aprroximately 3–4 times higher than for the virgin structure.

Closer values of the maximum softenings $\delta_{M,i}$ in the first mode and in the second mode of the structure indicate that all the storeys have damage and this is also supported by the visual inspections. Visual inspections, maximum softenings and the static damage indicator $\delta_{S,i}$ are compatible with each other after EQ1. After EQ2 and EQ3 there were differences between visual inspections and the $\delta_{S,i}$ damage indicators. The reason for these differences is that when local damage such as hinges occur the loss of stiffness becomes more clear at a certain distance from the actual location of the damage. For example, when a hinge develops in the fourth storey the apparent stiffness of the fifth storey may decrease significantly which can express more damage and increase the displacements in the fifth storey.

Fig. 18. Photos of all nodes in frame AAUWb.

Table 9. Damage classifications after the three earthquake events for frame AAUW

Storey	Frame	EQ1	EQ2	EQ3
1	AAUWa/AAUWb	UD/CR	CR/LD	SD/SD
2	AAUWa/AAUWb	UD/CR	CR/CR	LD/D
3	AAUWa/AAUWb	CR/UD	LD/CR	LD/D
4	AAUWa/AAUWb	CR/CR	CR/CR	SD/SD
5	AAUWa/AAUWb	UD/UD	CR/CR	SD/SD
6	AAUWa/AAUWb	UD/CR	CR/CR	CR/LD

9 CONCLUSIONS

In this paper the results of a series of shaking table tests with a model test 6-storey frame structure designed with a weak fourth storey have been presented. The weak storey was obtained by reducing the amount of reinforcement and using a poorer quality steel. In the undamaged structure the horizontal stiffness of the weak storey was found to be approximately 50% of the stiffness in the remaining storeys, in terms of less strength and stiffness.

The general conclusion from this study is that a weak storey in terms of changes in reinforcement did not have any significant effect on the dynamic displacements of the structure since no significant increases were seen in the inter-storey displacement of the weak storey. Furthermore, the mode shapes also did not show any signs of reduction in stiffness in the fourth storey. From visual inspection of the structure after the last earthquake, the fourth storey was found to be severely damaged, e.g. the mid-columns in both frames were having hinge-like joints to the third and the fifth storeys and shear-cuts where the maximum shear force is supposed to be. The damage evaluation from static tests showed a very low stiffness in the fourth storey after the last earthquake, but the relative change in stiffness was almost identical in all storeys. This observation is also supported by the evaluated mode shapes which almost remain unchanged even though a large reduction in stiffness is observed. The reason for failure in the weak storey is the low absolute stiffness in the weak storey which leads to large plastic deformations appearing as damage in the structure. It is concluded that failure occurs when the stiffness reaches a critical value and the storey is no longer able to transfer the shear forces from the storeys above.

From the test performed in this study, it can be concluded that structures having weak mid-storeys have a tendency to develop severe damage in these storeys and this also affects the behaviour and the magnitude of the displacements, especially in the storeys above the weak storey where severe damage was found as well.

ACKNOWLEDGEMENTS

REFERENCES

1. Banon, H., Biggs, J.M. & Irvine, H.M. Seismic damage in reinforced concrete frames. *Journal of the Structural Division, Proc. ASCE*, 1981, **107**(ST9), 1713–1729.
2. Stubbs, N. & Osegueda, R. Damage detection in periodic structures. *Damage Mechanics and Continuum Mechanics, ASCE*, 1985, **October**.
3. Penny, J.E.T., Wilson, D.A.L., Friswell, M.I., Damage Location in Structures using Vibration Data, Aston University, Birmingham, 1993.
4. Casas, J.R. Structural damage identification from dynamic-test data. *ASCE J. Struc. Eng.*, 1994, **120**(8), 2437–2450.
5. DiPasquale, E. & Çakmak, A.Ş. Detection of seismic structural damage using parameter-based global damage indices. *Probabilistic Engineering Mechanics*, 1990, **5**(2), 60–65.
6. Hassotis, S. & Jeong, G.D. Assessment of structural damage from natural frequency measurements. *Computers and Structures*, 1993, **49**(4), 679–691.
7. Koh, C.G., See, L.M. & Balendra, T. Damage detection of buildings: numerical and experimental studies. *ASCE J. Struc. Eng.*, 1995, **121**(8), 1155–1160.
8. Pandey, A.K. & Biswas, M. Damage detection in structures using changes in flexibility. *Journal of Sound and Vibration*, 1994, **169**(1), 3–17.
9. Park, Y.J. & Ang, A.H.-S. Mechanistic seismic damage model for reinforced concrete. *ASCE J. Struc. Eng.*, 1985, **111**(4), 722–739.
10. Park, Y.J., Ang, A.H.-S. & Wen, Y.K. Seismic damage analysis of reinforced concrete buildings. *ASCE J. Struc. Eng.*, 1985, **111**(4), 740–757.
11. Reinhorn, A.M., Seidel, M.J., Kunnath, S.K., Park, Y.J., Damage Assessment of Reinforced Concrete Structures in Eastern United States, NCEER-88-0016 Technical Report, June 1988.
12. Rodriguez-Gomez, S., Evaluation of seismic damage indices for reinforced concrete structures, M.Sc. Thesis, Princeton University, Princeton, NJ, October 1990.
13. Skjærbæk, P.S., Nielsen, S.R.K., Çakmak, A.S., Assessment of damage in seismically excited RC-structures from a single measured response, Proceedings of the 14th IMAC, Dearborn, MI, 12–15 February 1996, pp. 133–139.
14. Skjærbæk, P.S., Çakmak, A.S. & Nielsen, S.R.K. Identification of damage in RC-structures from earthquake records—optimal location of sensors. *Journal of Soil Dynamics and Earthquake Engineering*, 1996, **15**(6), 347–358.
15. Stephens, J.E. & Yao, J.P.T. Damage assessment using response measurements. *ASCE J. Struc. Eng.*, 1987, **113**(4), 787–801.
16. Stephens, J.E., Structural damage assessment using response measurements, Ph.D. Thesis, Purdue University, 1985.
17. Vestroni, F., Cerri, M.N., Antonacci, E., Damage detection in vibrating structures, in: Augusti, Borri, Spinelli (Eds.), Proceedings of Structural Dynamics-EURODYN'96, Torino, Italy, 1996, pp. 41–50.
18. Skjærbæk, P.S., Damage assessment of RC-structures subject to earthquakes, Ph.D. Thesis, Aalborg University, Denmark, 1997. Fracture and Dynamics, Paper No. 90.
19. Köylüoğlu, H.U., Nielsen, S.R.K., Çakmak, A.Ş., Local and modal damage indicators for reinforced concrete shear frames subject to earthquakes, submitted to Journal of Engineering Mechanics, ASCE, 1996.
20. Köylüoğlu, H.U., Nielsen, S.R.K. & Çakmak, A.Ş. Midbroken reinforced shear frames due to earthquakes. a hysteretic model to quantify damage at the storey level. *Soil Dynamics and Earthquake Engineering*, 1997, **16**, 95–112.
21. Pandit, S.M., Wu, S.M., Time Series and Systems Analysis with Applications, Wiley, 1983.
22. Juang, J.-N., Applied System Identification, Prentice Hall, Englewoods Cliffs, NJ, 1994.
23. Vold, H., Crowley, J., A modal confidence factor for the polyreference method, in: Proceedings of the 3rd International Modal Analysis Conference, 1984, pp. 305–310.
24. Kirkegaard, P.H., Andersen, P., Brincker, R., Identification of civil engineering structures using multivariate Armav and Rarmav models, presented at the International Conference on Identification in Engineering Systems, Swansea, 27–29 March 1996.

25. Kirkegaard, P.H., Skjærbæk, P.S., Andersen, P., Identification of time-varying civil engineering structures using multivariate recursive time domain models, in: Proceedings of the 21st international Symposium on Noise and Vibrations, ISMA21, Leuven, Belgium, 18–20 September 1996.

26. DiPasquale, E., Çakmak, A.Ş., Damage Assesment from Earthquake Records. Structures and Stochastic Methods, Elsevier, Amsterdam, pp. 123–138.

27. Nielsen, S.R.K., Köylüoğlu, H.U. & Çakmak, A.Ş. One and two-dimensional maximum softening damage indicators for reinforced concrete structures under seismic excitation. *Soil Dynamics and Earthquake Engineering*, 1992, **11**, 435–443.

28. Nielsen, S.R.K., Çakmak, A.Ş., Evaluation of maximum softening damage indicator for reinforced concrete under seismic excitation, in: Spanos, Brebbia (Eds.), Proceedings of the First International Conference on Computional Stochastic Mechanics, 1992, pp. 169–184, SS.